

# Submerged Membrane Breakwaters I: A Rahmen Type System Composed of Horizontal and Vertical Membranes

SUNG-TAE KEE\*

\*Civil Engineering Dept, Seoul National University of Technology, Seoul, Korea

## 수중 유연막 방파제 I : 수평-수직 유연막으로 구성된 라멘형 시스템

기성태\*

\*서울산업대학교 토목공학과

**KEY WORDS:** Flexible Prou-Membrane 유공 유연막, Wave-Flexible Structure Interaction 유연 구조 상호작용, Oblique Waves 경사파, Boundary Element Method 경계요소법

**ABSTRACT:** In the present paper, the hydrodynamics properties of a Rahmen type flexible porous breakwater interacting with obliquely or normally incident small amplitude waves are numerically investigated. This system is composed of dual vertical porous membranes hinged at the side edges of a submerged horizontal membrane. The dual vertical membranes are extended downward and hinged at seabed. The effects of permeability, Rahmen type membrane breakwater geometry, pre-tensions on membranes, relative dimensionless wave number, and incident wave headings are thoroughly examined.

### 1. Introduction

The flexible and porous structures can be used as breakwater to effectively reduce both the transmitted and reflected wave heights. The two-dimensional problem of wave interaction with porous flexible structure is of growing importance and significant studies in this area have been conducted by several authors.

The problem of the reflection and transmission of small amplitude waves by a flexible, porous, and thin beam-like breakwater has been treated by Wang and Ren (1993a). Wang and Ren (1993b) have also studied the wave-trapping effect due to a flexible porous breakwater located in front of a vertical impermeable wall. Yu and Chang (1994) investigated the interaction of surface waves with a submerged horizontal porous plate. Cho and Kim (2000) studied the interaction of monochromatic incident waves with a horizontal porous flexible membrane in the context of two-dimensional linear hydro-elastic theory, and found that using a proper porous material can further enhance the overall performance of the horizontal flexible membrane.

The interaction of monochromatic incident wave with dual

pre-tensioned, inextensible, vertical nonporous-membrane wave barrier extending the entire water depth has been investigated by Edmond (1998) using eigenfunction expansions for the velocity potential and linear membrane theory. Cho et al. (1998) developed an analytic solution for dual nonporous-membrane system and a boundary integral method solution for more practical dual buoy/membrane wave barriers with either surface piercing or fully submerged system in oblique seas.

In the present paper, the hydrodynamics properties of a Rahman type porous membranes interacting with obliquely incident small amplitude waves are numerically investigated. This system is composed of one submerged horizontal porous flexible membrane and two vertical porous membranes hinged at the both side edges of horizontal membrane. The two vertical membranes hinged at edges of horizontal membranes are extended downward, and hinged at seabed. The fully submerged Rahmen type breakwater is introduced herein in the points of view of marine scenario, water circulation, surface vessel passing, and the reduced hydrodynamic pressures on the body of structures.

To assess the efficiency of this Rahmen type porous membranes system, two-dimensional hydro-elastic formulation for two fluid domains was carried out in the context of linear wave-body interaction theory and Darcy's law. The fluid region is split into two regions, region (1)

제1저자 기성태 연락처 : 서울시 노원구 공릉동 172  
02-970-6509 stkee@snut.ac.kr

wave ward, over and in the lee of the structure, and region (2) inside of the structure. It is assumed, for simplicity, that the pre-tensioned membrane is thin, un-stretchable, and free to move only in the transverse direction for vertical membranes, and in the longitudinal direction for the horizontal membrane. The pre-tension is assumed externally provided and much greater than dynamic tension. The membrane dynamics is modeled as that of the tensioned string of zero bending rigidity. The velocity potentials of wave motion are fully coupled with deformations of membranes taking account for the porosity based on Darcy's law.

The numerical model is validated by comparison with previously published numerical studies by Cho and Kim (2000) based on eigenfunction expansion of the limiting cases of the horizontal porous membrane in monochromatic waves. Relevant numerical results that are presented relate to the reflection and transmission coefficients. The corresponding wave forces and motions of membranes are also investigated, but not presented here. The effects of permeability, Rahmen type membrane breakwater geometry, pre-tensions on membranes, relative dimensionless wave number, and incident wave headings are thoroughly examined.

Results presented herein confirm that the overall performance of the Rahmen type flexible membranes can be further enhanced by using a proper porous material, since the inclusion of permeability on membrane eliminates the resonance that aggravates the breakwater performance. The performance of this type of breakwater is found to be highly promising for wide range of frequency and wave headings if it is properly tuned to the coming waves using Rahmens geometry, pre-tensions, and permeability.

## 2. Theory and Numerical Method

### 2.1 Governing Equations

The breakwater system with arbitrary porous and flexible boundaries is to compose of a horizontal membrane with width of  $W$  submerged downward a distance  $D$  below the still water level and two vertical membranes extended to sea bottom. The sketch diagram is shown in Fig. 1. A Cartesian coordinate system  $(x, y)$  is defined with  $x$  measured in the direction of wave propagation from a point mid-way between the vertical membranes, and  $y$  measure upward from the still water level. An obliquely incident, regular, small amplitude wave train of half height  $A$  and angular frequency  $\omega$  propagates towards the breakwater with an angle  $\theta$  with respect to  $x$  axis in water of constant depth  $h$  as shown in Fig. 1.

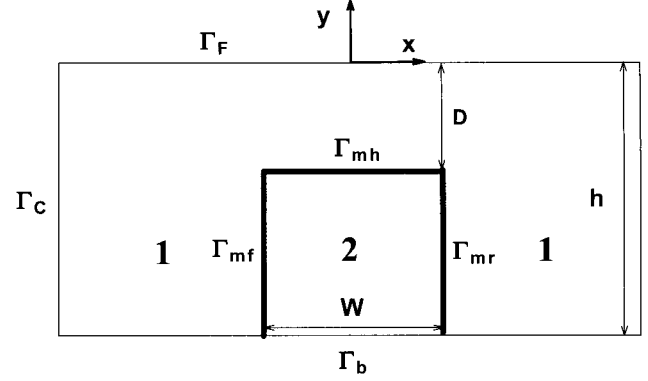


Fig. 1 Definition sketch and integration domains for Rahman type porous membrane breakwater.

If the fluid is assumed incompressible, inviscid, and the flow irrotational, then the fluid motion can be described by velocity potential  $\Phi$  that satisfies the Helmholtz equation  $\nabla^2 \phi_l - k_z^2 \phi_l = 0$  within the fluid regions ( $\Omega_l$ ,  $l=1, 2$ ). In addition, the wave amplitude is assumed sufficiently small enough for linear wave theory to apply. Consequently,  $\Phi$  is subject to the usual boundary conditions, linearized free surface ( $\Gamma_F$ ), bottom ( $\Gamma_b$ ), and approximated far field conditions ( $\Gamma_C$ ): (see, for example, Sarpkaya and Issacson, 1981). Thus  $\Phi$  may be expressed in the flowing form:

$$\Phi(x, y, z, t) = \text{Re}[\{\phi_o(x, y) + \phi_l(x, y)\} e^{ik_z z - i\omega t}] \quad (1)$$

where  $\phi_o$  is the well-known incident potential, and can be written as;

$$\phi_o = \frac{igA}{\omega} \frac{\cosh k_o(y+h)}{\cosh k_o h} e^{ik_o \cos \theta x} \quad (2)$$

Also,  $\text{Re}[\ ]$  denotes the real part of a complex expression,  $i = \sqrt{-1}$ ,  $t$  denotes time, and  $k_z = k_o \sin \theta$  is the wave number component in the  $z$  direction. The wave number of the incident wave  $k_o$  is the positive real solution of the dispersion equation  $\omega^2 = k_o g \tanh k_o h$  with  $g$  being the gravitational constant. And  $\phi_l$  is time-independent unknown scattered potentials in two fluid domains (see Fig. 1) includes both effects of diffraction and radiation.

### 2.2 Permeable Membrane Boundary Condition

The required linearized kinematic boundary condition on the surface of the permeable flexible structure may be developed based on the formulation of Wang and Ren (1993a). This may be expressed for vertical membranes as:

$$\frac{\partial \phi_1}{\partial x} = - \frac{\partial \phi_2}{\partial x} = -i\omega \xi + u(y) \quad (3)$$

where  $u(y)$  is spatial component of the normal velocity  $U(y, t)$  of the fluid flow passing through a thin porous media, which is assumed to obey Darcy's law. The harmonic membrane motion is  $Re[\xi e^{-i\omega t}]$ . The porous flow velocity from fluid region 1 to region 2,  $U(y, t) = Re[u(y) e^{-i\omega t}]$  linearly relates the pressure difference across the thin porous membrane. Therefore, it follows that

$$U(y, t) = \frac{B}{\mu} (p_1 - p_2) = \frac{B}{\mu} \rho i \omega (\phi_1 - \phi_2) e^{-i\omega t} \quad (4)$$

where  $B$  is the constant called permeability having dimension of a length,  $\mu$  is constant coefficient of dynamic viscosity, and  $\rho$  is constant fluid density. From Eqs. (3) and (4),  $u(y)$  has an expression as follows:

$$u(y) = \frac{B}{\mu} \rho i \omega (\phi_1 - \phi_2) \quad (5)$$

In order to match the two solutions on the surface of permeable membranes,  $\phi$  and  $\xi$ , the scattered potentials must also satisfy the following linearized dynamic boundary conditions on the membrane surface:

$$\frac{d^2 \xi}{dy^2} + \lambda^2 \xi = -\frac{\rho i \omega}{T} (\phi_1 - \phi_2) \quad (\text{on } \Gamma_m) \quad (6)$$

where  $\lambda = \omega/c$ , and  $c$  is membrane wave speed given by  $\sqrt{T/m}$  with  $T$  and  $m$  being the membrane tension and mass per unit length respectively.

### 2.3 Boundary Integral Equation

The fundamental solution (Green function) of the Helmholtz equation and its the normal derivative of  $G$  are given using the modified zeroth  $K_0(\lambda r)$  and first order  $K_1(\lambda r)$  Bessel function of the second kind (see, for example, Rahman and Chen, 1993), and where  $r$  is the distance from source point to the field point. After imposing the boundary conditions, the integral equations in fluid domain can be written as

$$\begin{aligned} C\phi_1 + \int_{\Gamma_f} [k_z K_1(k_z r) \frac{\partial r}{\partial n} - \nu K_0(k_z r)] \phi_1 d\Gamma \\ + \int_{\Gamma_c} [k_z K_1(k_z r) \frac{\partial r}{\partial n} - ik_x K_0(k_z r)] \phi_1 d\Gamma \\ + \int_{\Gamma_m} [\phi_1 k_z K_1(k_z r) \frac{\partial r}{\partial n} + \frac{B}{\mu} i \rho \omega K_0(k_z r) (\phi_2 - \phi_1) \\ + s l_{jnr} i \omega \xi K_0(k_z r)] d\Gamma + \int_{\Gamma_b} \phi_1 k_z K_1(k_z r) \frac{\partial r}{\partial n} d\Gamma \\ = - \int_{\Gamma_m} K_0(k_z r) (\frac{\partial \phi_o}{\partial n} + i \rho \omega \frac{B}{\mu} \phi_o) d\Gamma \quad (\text{in } \Omega_1) \end{aligned} \quad (7)$$

$$\begin{aligned} C\phi_2 + \int_{\Gamma_m} [\phi_2 k_z K_1(k_z r) \frac{\partial r}{\partial n} + \frac{B}{\mu} i \rho \omega K_0(k_z r) (\phi_1 - \phi_2) \\ - s l_{jnr} i \omega \xi K_0(k_z r)] d\Gamma + \int_{\Gamma_b} \phi_2 k_z K_1(k_z r) \frac{\partial r}{\partial n} d\Gamma \\ = - \int_{\Gamma_m} K_0(k_z r) i \rho \omega \frac{B}{\mu} \phi_o d\Gamma \quad (\text{in } \Omega_2) \end{aligned} \quad (8)$$

where  $C$  is solid-angle constant, and  $\nu = \omega^2/g$  is the infinite-depth dimensionless wave number,  $s l_{jnr} = -, +, +, +$ ,  $s l_{jnr} = +, -, -$  for front vertical, horizontal, rear vertical membrane respectively.

The integral equations (7-8) can then be transformed to the corresponding algebraic matrix. The entire boundary is discretized into a large finite number of segments, and can be replaced by  $N \times N$  matrix equations. Then,  $N$  includes numbers of segments along all boundaries, and there exist  $N$  unknowns for  $\phi_1, \phi_2, N_{mf}, N_{mh}, N_{mr}$  for membrane motions, which can be given in discrete form for each segment (see, for example, Kim and Kee, 1996).

### 3. Numerical Results and Discussions

A boundary integral equation method based on the distribution of simple sources along the entire boundary is developed for the numerical solution. The two vertical truncation boundaries are located sufficiently far from the membrane such that far field boundary condition is valid, i.e. to ensure that local wave effect is negligible.

Considering the phase velocity of incident wave ( $\omega/k_x$ ) and a measure of porosity with length dimension ( $B$ ), the defined dimensionless porosity ( $2\pi\rho\omega B/k_x\mu$ ) by Cho and Kim (2000) can be regarded as a sort of Reynolds number representing the effects of both viscosity and porosity.

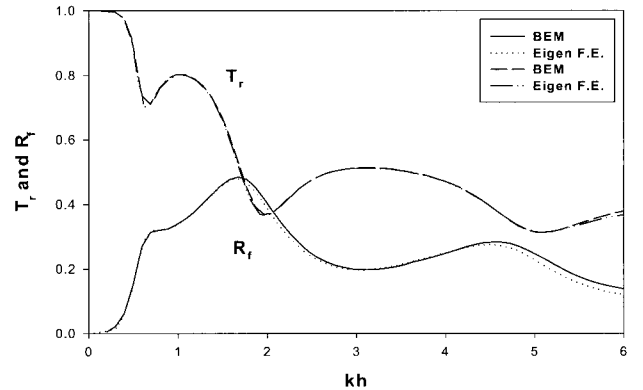


Fig. 2 Comparison of numerical method with analytic solutions.

The results are for  $D/h = 0.2$ ,  $W/h = 1.0$ ,  $\theta = 0^\circ$ ,

$T_h = 0.1$ ,  $2\pi\rho\omega B/k_x\mu = 2.0$

The numerical results were checked against the energy conservation formula i.e.  $R_f^2 + T_r^2 = 1$ , since the energy relation is satisfied in the case of zero porosity (or an impermeable membrane). For further verification, a submerged horizontal membrane case is considered. For this horizontal system, analytic solution has been developed for monochromatic incident wave by Cho and Kim (2000), and is compared to numerical results with good agreement as shown in Fig. 2. For two vertical non-porous membrane systems without horizontal membrane, the comparison of numerical results and analytical solution had been checked in the previous study (Cho et al., 1998).

Transmission and reflection coefficient as function of  $kh$  for the various permeability parameters  $B=0, 1E-09, 5E-09, 1E-08, 5E-08, 1E-07, 5E-07, 1E-06$  for a beam sea ( $\theta=0^\circ$ ) and dimensionless pre-tensions of membrane ( $\mathcal{T}$ ) are shown in Figs. 3-4. The externally provided tension of membrane is normalized by  $\rho gh^2$ , i.e.  $\mathcal{T} = T / \rho gh^2$ . The symbols  $\mathcal{T}_f, \mathcal{T}_h, \mathcal{T}_r$  represent the non-dimensional pre-tensions for a front vertical, a horizontal, and a rear vertical membrane respectively. The reflected and transmitted wave is gradually decreased as permeability parameter  $B$  increases.

However, the transmitted wave for permeability coefficients higher than  $1E-07$  is increased over the entire incident wave frequencies. Similar phenomena occur in the energy relation shown in Fig. 5. The error of energy relation is decreased for the permeability higher than  $1E-07$ . Thus, it is of particular interest to note that the best wave energy dissipation in harmonics with hydrodynamics of membranes occurs for a system has the permeability coefficient  $1E-07$  on the membrane surfaces. For a higher permeability over the  $B=1E-07$ , improperly large transmitted waves surpass the wave blocking efficiency by the hydrodynamic

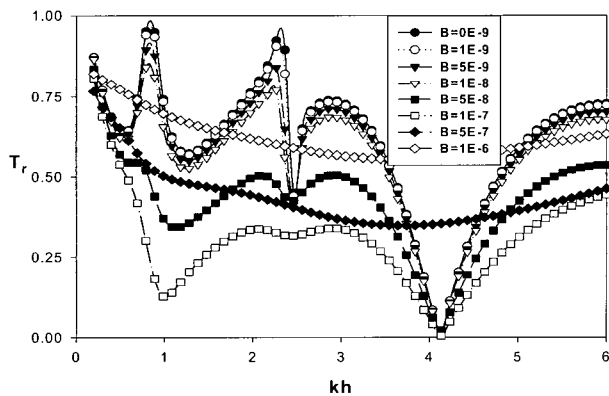


Fig. 3 Transmission Coefficient for  $D/h=0.2, W/h=1.0, \theta=0^\circ$  and  $\mathcal{T}_f=0.1, \mathcal{T}_h=0.05, \mathcal{T}_r=0.1$

effects of flexible system. This could be a validation for the assumption that the permeability is not too high (say less than  $B=1E-07 m^2$ ) by Kim et al. (2000) to solve the wave interaction with arbitrary porous and rigid boundaries based on potential theory and Darcy's law. Thus, the permeability  $B=1E-07$  can be defined as an effective porosity that causes maximum energy dissipation on the system as shown in Fig. 5.

The performance of Rahmen type wave barrier should depend on various design parameters, such as membrane parameters, submergence depth, width, and incident wave angle and frequencies. First, the performance of Rahmen type

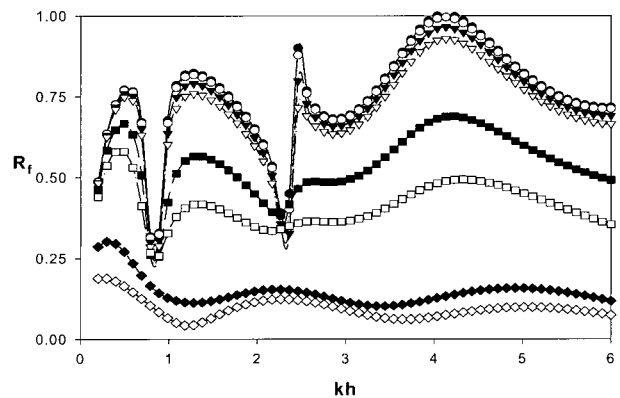


Fig. 4 Reflection Coefficient for  $D/h=0.2, W/h=1.0, \theta=0^\circ$  and  $\mathcal{T}_f=0.1, \mathcal{T}_h=0.05, \mathcal{T}_r=0.1$

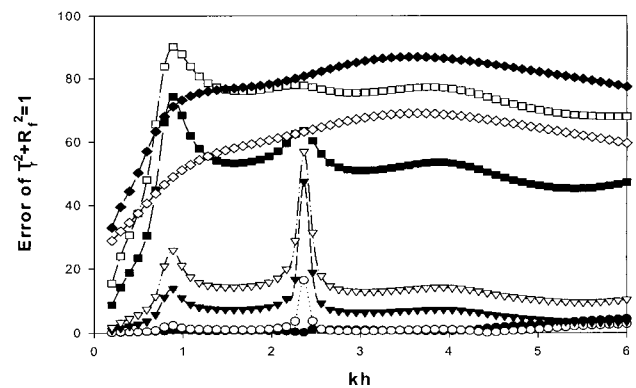
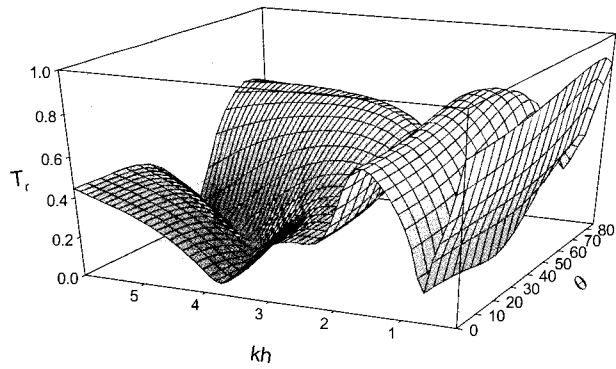


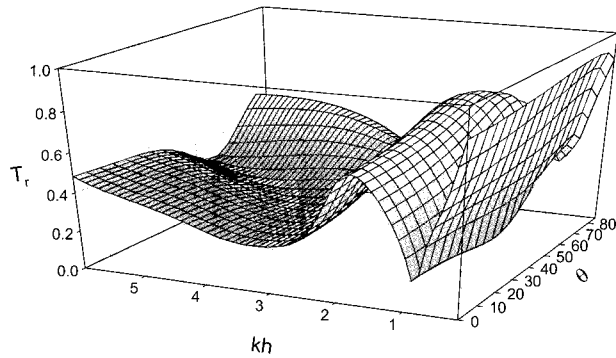
Fig. 5 Energy relation error for  $D/h=0.2, W/h=1.0, \theta=0^\circ$  and  $\mathcal{T}_f=0.1, \mathcal{T}_h=0.05, \mathcal{T}_r=0.1$

wave barriers for various submergence depths after imposing the same permeability  $B=1E-07$  on two vertical and one horizontal membrane is shown in Fig. 6a-6c for various wave headings and dimensionless frequencies. The dimensionless pre-tensions of front, horizontal, and rear membranes assumed to be given externally as  $\mathcal{T}_{f,h,r}=0.05$ .

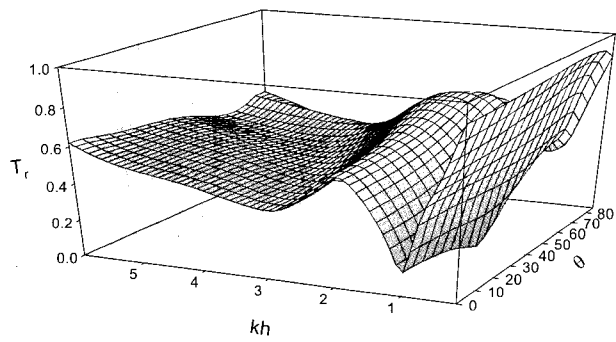
In Fig. 6a, the case of  $D/h=0.2$  shows the lowest transmission in the region of  $2.0 \leq kh \leq 5.5$  and  $0^\circ \leq \theta \leq 55^\circ$ . As the submergence depth ratio is increased to  $D/h=0.25$  (Fig. 6b) and  $D/h=0.3$  (Fig. 6c), the performance become worse in the region of  $2.0 \leq kh \leq 5.5$  and  $0^\circ \leq \theta \leq 55^\circ$  due to less wave breaking efficiency by the reduced height of vertical membranes occupying water column. However, the performance is not sensitive to the change in the submergence depth in the long-wave regime.



(a)  $D/h=0.2$



(b)  $D/h=0.25$

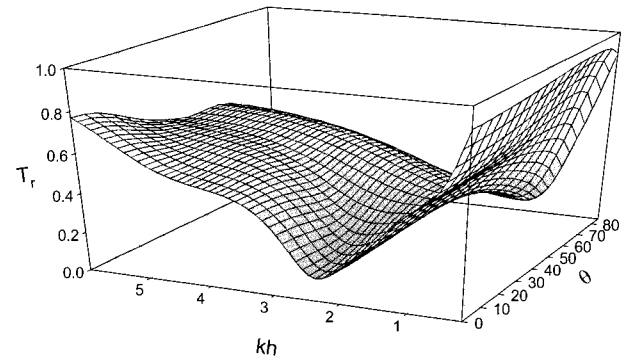


(c)  $D/h=0.3$

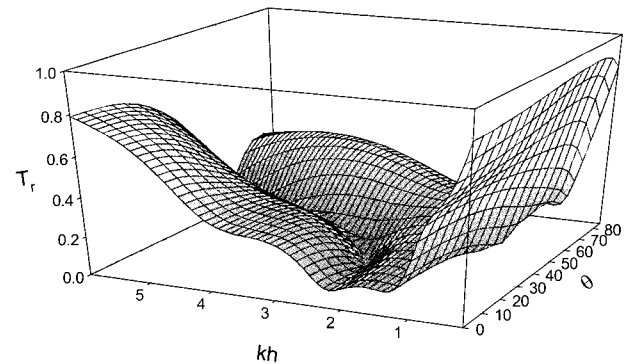
Fig. 6 Transmission coefficients for  $W/h=1.0$ ,  $\tilde{T}_{f,h,r} = 0.05$ ,  $B=1E-07$

Figs. 7a~7c show transmission coefficients against a dimensionless wave number for various size of width of system with pre-tensions of flexible membranes  $\tilde{T}_{f,h,r} = 0.05, 0.1, 0.15$ . The larger size of system is expected to allow less transmission in the wide range of frequencies and headings.

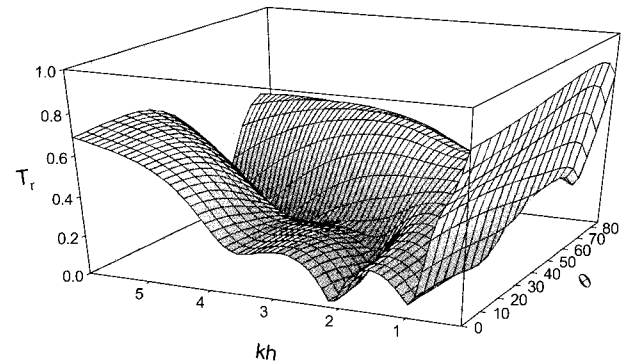
However, the performance of system with  $W/h=1.0$  is better than that of  $W/h=1.25$  except in the narrow range of high frequencies and low headings. This example typically shows that a larger size of system does not ensnare warrant better performance. Highly flexible



(a)  $W/h=0.75$



(b)  $W/h=1.0$



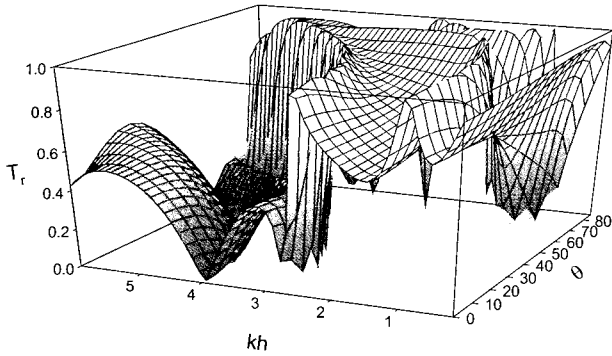
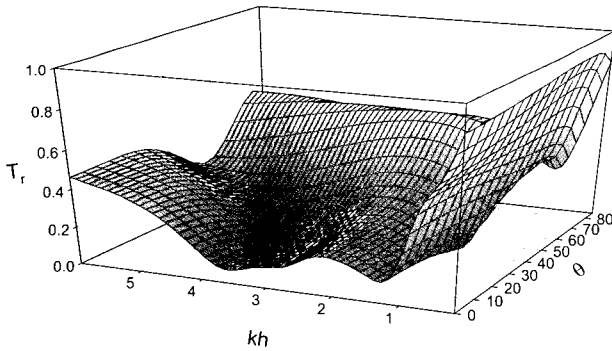
(c)  $W/h=1.25$

Fig. 7 Transmission coefficients for  $D/h=0.25$ ,  $\tilde{T}_{f,h,r} = 0.05, 0.1, 0.15$  and  $B=1E-07$

horizontal membrane allows large fluctuating motion that generate radiated waves for mutual cancellations against the incident waves, and has better wave blocking performance at given submergence depth.

Figs. 8a-8b show transmission coefficients against a dimensionless wave number for a system with pre-tensions of flexible membranes  $\bar{T}_{f,h,r} = 0.1, 0.05, 0.1$ . In Fig. 8a, the system with permeability  $B=0$  shows good performance in the half-arch range of frequencies along  $kh \geq 2.8$  and  $0^\circ \leq \theta \leq 75^\circ$ . It is interesting to note that the frequency region ensuring good performance is migrated to higher frequency as wave heading is increased, which is due to shorter wavelength for the high angle of attack by oblique incident waves. In the region of low frequencies, almost complete transmissions are occurred, which mainly due to the large fluctuating motion of membranes that generate waves in the lee side instead of mutual cancellation against the incident waves. After imposing the permeability  $B=1E-07$  on membranes, the performance of system is dramatically improved in the wide range of frequencies and wave headings  $0^\circ \leq \theta \leq 75^\circ$  in Fig. 8b.

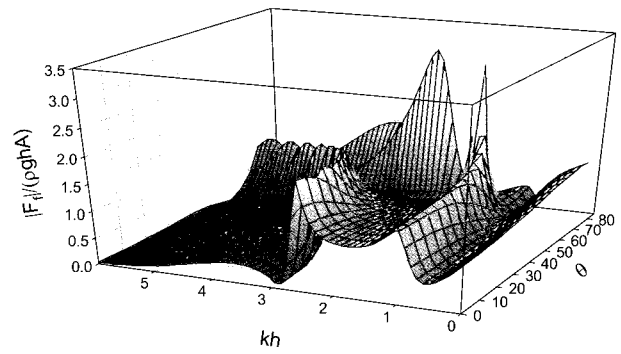
In Figs. 9, the distribution trend of dimensionless hydrodynamic forces on front and rear membranes closely matched to the shapes of transmission coefficients in Fig. 8a.

(a)  $B=0$ (b)  $B=1E-7$ 

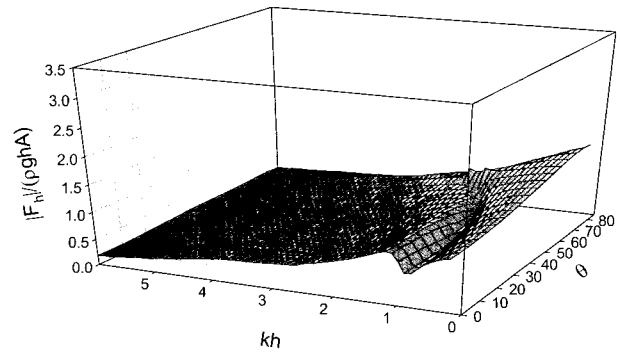
**Fig. 8** Transmission coefficients for  $W/h=1.0, D/h=0.25, \bar{T}_{f,h,r}=0.1, 0.05, 0.1$  and  $B=1E-07$

The effects of membrane porosity on the wave-blocking performance are vividly manifested in Fig. 8b.

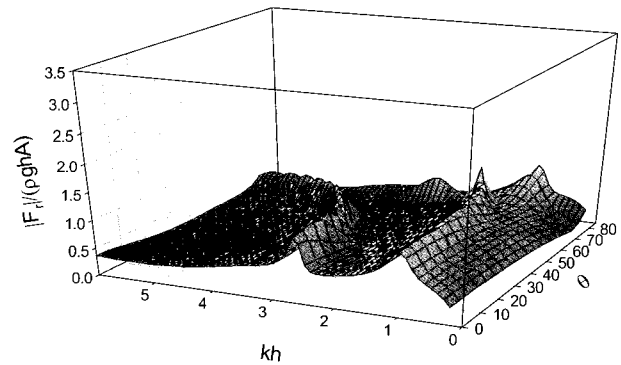
In the case of porous membrane, there is wave energy dissipation through pore pores due to fluid viscosity. Thus, the wave transmission over the effective porous membranes is significantly smaller compared to the impermeable case due to viscous dissipation. The generally similar trend for  $\theta=0^\circ$  has been occurred in the motions amplitudes of impermeable and porous membranes in Fig. 10~11.



(a) Front membrane



(b) Horizontal membrane

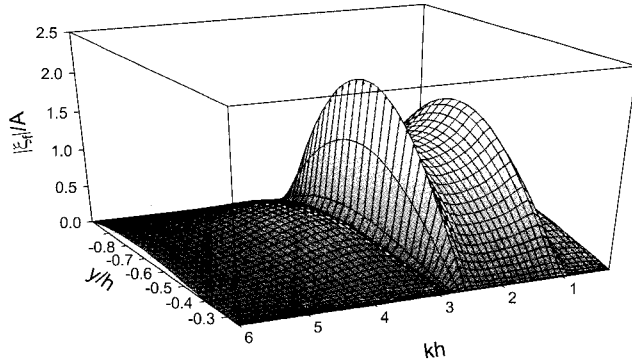


(c) Rear membrane

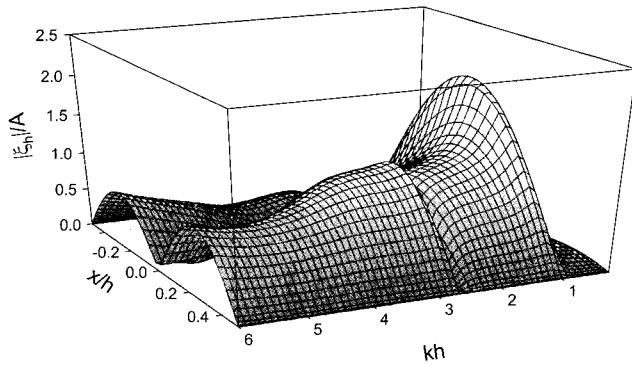
**Fig. 9** Dimensionless force distribution on membranes as function of  $kh$  and  $\theta$  for  $\bar{T}_{f,h,r}=0.1, 0.05, 0.1, W/h=1.0, D/h=0.25, B=0$

The large motions of membranes at the frequencies  $kh=1.2$  and  $kh=2.8$  relates to the poor performances as wave barrier in Fig. 8a. In the motions of horizontal membrane that does not directly block incoming wave, higher modes start to appear as wavelength becomes shorter.

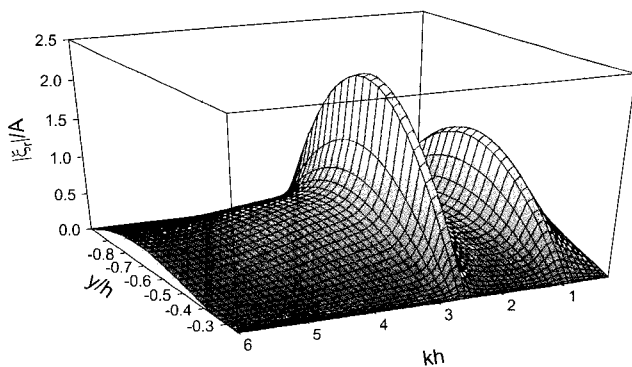
This phenomenon at the shorter wavelength region seems to be related to the high efficiency as wave barrier due to



(a) Front membrane



(b) Horizontal membrane



(c) Rear membrane

Fig. 10 Response of membrane as function of  $kh$  and  $y/h$  for  $\theta=0^\circ$ ,  $\bar{T}_{f,h,r}=0.1, 0.05, 0.1$ ,  $W/h=1.0$ ,  $D/h=0.25$ ,  $B=0$

favorable phase cancellation and smaller motion-induced waves in the lee side as shown in Fig 8a.

When the permeability is introduced on membranes, for example, the maximum response amplitudes for rear membrane are significantly reduced as shown in Fig. 11. This wave energy dissipation through pores seems to be directly related to excellent wave-blocking efficiency.

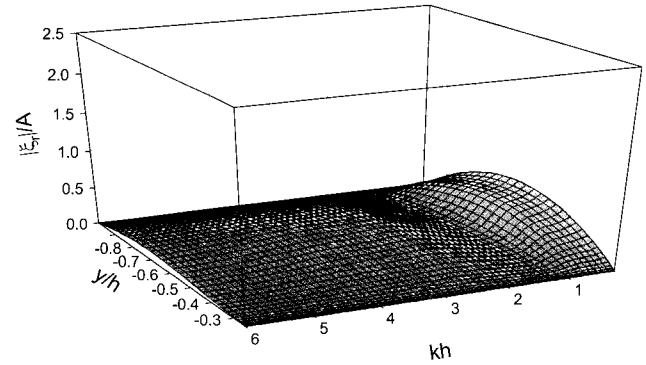


Fig. 11 Response of a rear membrane as function of  $kh$  and  $y/h$  for  $\theta=0^\circ$ ,  $\bar{T}_{f,h,r}=0.1, 0.05, 0.1$ ,  $W/h=1.0$ ,  $D/h=0.25$ ,  $B=1E-07$

The effects of membrane porosity can be either positive or negative depending on the given wave condition and system design parameters. Thus, at a certain frequency, for example around  $kh=4.0$  in Fig 8a-8b, the efficiency can worsen by using porous membranes. However, the overall efficiency of porous membrane system can be achieved along the wide frequencies and headings by optimal combination of design parameters.

#### 4. Summary and Conclusions

The interaction of oblique incident waves with a Rahman type porous flexible membrane breakwater was investigated in the context of 2D linear hydroelastic theory. The viscous flow effects around fine pores on membranes were accounted for through Darcy's law. Properly adjusted 2-D B.E.M. code has been developed for the performance analysis of fully submerged Rahman type system. The developed program has been checked against the analytic solution for limited cases in good agreement. Using the developed program, the performance was investigated for the various submergence depth, width of horizontal membrane, pre-tensions, permeability, and wave conditions. Based on the results analysis, it is found that the optimal system with an effective permeability coefficient can significantly improve the overall performances as wave barrier along the wide range of incident waves frequencies and headings.

### Acknowledgment

This research was sponsored by the Korea Research Foundation (KRF), Grant Number E00599.

### References

- Cho, I.H., Kee, S.T. and Kim, M.H. (1998). "The Performance of Dual Flexible Membrane Wave Barrier in Oblique Sea" ASCE J. of Waterways, Port, Coastal & Ocean Engineering, Vol 124, No 1, pp 21-30.
- Cho, I.H. and Kim, M.H. (2000). "Interactions of Horizontal Porous Flexible Membrane with Waves." ASCE J. of Waterway, Port, Coastal & Ocean Engineering, Vol 126, No 5, pp 245-253.
- Edmond, Y.M. (1998). "Flexible Dual Membrane Wave Barrier" ASCE J. of Waterway, Port, Coastal & Ocean Engineering, Vol 124, No 5, pp 264-271.
- Kim, M.H. and Kee, S.T. (1996). "Flexible Membrane Wave Barrier. Part 1. Analytic and Numerical Solutions" ASCE J. of Waterways, Port, Coastal & Ocean Engineering, Vol 122, No 1, pp 46-53.
- Kim, M.H., Koo, W.C. and Hong, S.Y. (2000). "Wave Interactions with 2D Structures On/Inside Porous Seabed by a Two-domain Boundary Element Method" Journal of Applied Ocean Research, Vol 22, pp 255-266.
- Rahman, M. and Chen., M. (1993). "Boundary Element Method for Diffraction of Oblique Waves by an Infinite Cylinder." Engineering Analysis with Boundary Elements, Vol 11, pp 17-24.
- Sarpkaya, T. and Isaacson, M. (1981). Mechanics of Wave Forces on Offshore Structures, Van Nostrand Reinhold, New York.
- Wang, K.H. and Ren, X. (1993a). "An Effective Wave-Trapping System," Ocean Engineering, Vol 21, pp 155-178.
- Wang, K.H. and Ren, X. (1993b). "Wave Motion Through Porous Structures." J. Engineering. Mech., ASCE, Vol 120, No 5, pp 989-1008.
- Yu, X and Chawang, A.T. (1994). "Water Waves Above a Submerged Porous Plate." J. Engrg. Mech., ASCE, Vol 120, No 5, pp 1270-1278.

---

2002년 6월 19일 원고 접수

2002년 9월 2일 수정본 채택